Enhanced Knowledge in Sciences and Technology Vol. 3 No. 2 (2023) 355-365

EKST

Homepage: http://publisher.uthm.edu.my/periodicals/index.php/ekst
e-ISSN : 2773-6385

The Physicochemical Characteristics of Oil Palm Residue-Clay Biocomposite for Removing Sunset Yellow in Water

Logithavani Padmanaban[1], Zalilah Murni Yunus[1]*

[1]Department of Technology and Natural Resources,
Faculty of Applied Sciences and Technology,
Universiti Tun Hussein Onn Malaysia (Pagoh Campus),
84600 Pagoh, Muar, Johor, MALAYSIA

*Corresponding Author Designation

DOI: https://doi.org/10.30880/ekst. 2023.03.02.041
Received 16 January 2023; Accepted 16 February 2023; Available online 30 November 2023

Abstract: The demand for synthetic food colouring in food industries has been increasing due to its low cost as compared to natural colourant. Sunset yellow (SY) is one of the most utilized synthetic food colourings in food industries to add colour into beverages, sweets, ice cream, jams, jelly, condiments and other foods. Presence of sunset yellow residues in discharge water from food industries is capable of harming living organism. Adsorption techniques by using biodegradable adsorbent have been used as an effective method to remove these contaminants from water. This research involves preparation of biochar derived from oil palm residue reinforced with clay as an inexpensive adsorbent for removing contaminants in waste water. The physicochemical characteristics of this clay biocomposite was investigated. The characterization of adsorbent has displayed the presence of functional groups by Fourier transform infrared spectroscopy (FTIR). The concentration of solution before and after the treatment with clay biocomposite were determined with Ultraviolet-Visible spectroscopy (UV-VIS). The maximum removal efficiency was observed at pH 4, 5 mg/L of solution concentration. The adsorption has reached equilibrium after 30 min of contact time between adsorbent and adsorbate. The pseudo-second kinetic order (R^2=0.981) and Langmuir isotherm model (R^2=0.9598) were well fitted to the adsorption data. The utilization of oil palm biomass into adsorbent could solve the oil palm biomass disposal issues and as an alternative solution for the sanitation of wastewater contaminated with sunset yellow.

Keywords: Biochar, Clay Biocomposite, Oil Palm Residue, Sunset Yellow

1. Introduction

Over time, the usage of synthetic organic dyes in food manufacturing has increased due to the dearth and expensive cost of natural colourants. Currently, artificial organic dyes make up the majority of all

*Corresponding author: zalilah@uthm.edu.my

colourants and are frequently used to add colour into the beverages, sweets, ice cream, jams, jelly, condiments, and other foods [1]. Industry-wide dyes are often divided into two groups: ionic (anionic and cationic) and nonionic [2]. Azo dyes are popular as commonly used food colorants because they are reliable and inexpensive [3]. However, many of these colours have the potential to harm living organisms, making it imperative to regulate their presence in food.

One of the most popular food colourings that has been utilized in food industries is Sunset Yellow (SY), a synthetic mono-azo dye which has a molecular structure of (-N=N-) that is used in a variety of foods [4]. Previous research has demonstrated that sunset yellow can have a variety of harmful health impacts, including thymus weight loss, changes to reproductive and neurobehavioral characteristics [5]. Higher levels exposure of sunset yellow in people may put the torso at risk for serious conditions such hyperactivity, thyroid cancer, asthma, lupus, eczema and migraines. Therefore, it is crucial to reduce or eliminate dye concentrations in effluents before being released into water bodies. In order to minimize the impact of food dye towards the environment, a variety of treatment methods have been employed, including microbial breakdown, photo-catalytic reduction, coagulation or flocculation, ion exchange, reverse osmosis, and adsorption approach. Among these several dye removal techniques, adsorption has been proven to be the most significant and trustworthy. It has also been found to be more cost-effective [7].

Oil palm waste acts as matrix material is currently utilized as biochar for the adsorption of dyes or colours from wastewater. The fibre acts as matrix material which is less expensive, excellent thermal properties, higher energy recovery and environment friendly. This study aimed to discover some new methods to make use of carbonaceous composite materials (Empty Oil Palm Fruit Bunch) for the removal of sunset yellow food colouring in water and to come up with acceptable reference for possible applications of biomass-derived activated carbon-based mineral composites, and thus enhance the effectiveness domination of both mineral and biomass resources.

2. Materials and Methods

2.1 Materials Specifications

Oil palm empty fruit bunch (OPEFB), clay (Ca-montmorillonite), 20% v/v Hydrochloric acid (HCl), distilled water, standard sunset yellow and commercial sunset yellow (Star Brand) were utilized in this study are

2.2 Methods

2.2.1 Sample Preparation

OPEFB was collected from Ladang Ambar, Senai (Johor). The empty fruit bunch (EFB) was dried thoroughly by sun drying. Dried EFB fiber (30 g) was treated with 20% v/v HCl overnight. In this study, chemically modified EFB fiber was carbonized in a muffle furnace at 389.73 ℃ for 2 hours at which the carbonization temperature was determined by thermal analysis (TGA) with a heat rate of 10 ◦C/min under 700 ◦C and 25 mL/min of nitrogen flow rate. EFB- based activated carbon (2 g) was mixed together with 12 g of clay (Ca-montmorillonite) in a ball milling machine [9].

2.2.2 Physicochemical analysis

FTIR spectrometry was used to examine the functional groups that present on the surface of the oil palm EFB and EFB-activated carbon. In this study, raw EFB, activated carbon, clay/biochar composite before and after the treatment were analysed with FTIR spectrometer with attenuated total reflectance (ATR) capability method in the range of 400–4000 cm^{-1}[10]. Thermogravimetric analysis (TGA) is a method that has been implemented to measure changes in the sample mass loss that is subjected to changing of temperature in controlled atmosphere condition [11]. Moisture drying, main devolatilization and continuous slight devolatilization are the three stages involved in mass loss due to raw EBF fiber pyrolysis in nitrogen gas [12]. In this study, less than 1 gram of EFB fibers were

pyrolyzed with nitrogen (25 mL/min) under 700 ◦C with a heating rate of 10 ◦C /min for 1 hour and 16 minutes.

2.2.2.1 pH study

Experiment was conducted on the sorption behaviour of clay/biochar composites with different pH ranges (4, 6, 8 and 10) that was maintained by 0.1 M of NaOH or HCl. Sunset yellow solution (25 mL) that had a concentration of 10 mg/L was shaken at 150 rpm for 120 minutes with the aid of magnetic stirrer at 298 K [13]. In this study, the concentration of sunset yellow in water before and after the treatment with adsorbent (clay/activated carbon) was analysed with UV-VIS spectrophotometer at maximum wavelength of 480.0 nm. The following formula were used to calculate the removal efficiency (%):

$$\boldsymbol{Removal\ efficiency}\ (\%) = \frac{(\boldsymbol{C_o - C_e})}{\boldsymbol{C_0}} \times \mathbf{100} \qquad \boldsymbol{Eq.1}$$

where C_o and C_e are initial and equilibrium concentrations (mg/L) of sunset yellow, respectively [14].

2.2.2.2 Adsorption kinetic study

The impact of contact time on sunset yellow adsorption toward clay biocomposite was calculated using a kinetic experiment. The adsorption experiment was conducted at different time intervals (2, 3, 5, 10, 15, 20, 25, 30, 40, and 50 min) at 298 K. From the 10 mg/L solutions, 10 mL of sunset yellow solution was shaken mechanically with a dosage of 0.01 g of clay biocomposite for 1 hour. Every experiment was repeated three times in triplicate, and the experimental data was presented as the mean of their results. The adsorption capacity of clay biocomposite is denoted by Qt (mg/g) along with the time (t) was calculated by using the following equation:

$$\mathbf{Q_t} = \frac{(\mathbf{C_o - C_t})\mathbf{v}}{\mathbf{w}} \qquad \mathbf{Eq.2}$$

where the adsorption capacity of clay biocomposite is denoted by Q_t (mg/g). The initial and final concentration of sunset yellow solution are denoted by C_0 and C_t, respectively (mg/L). The volume of solution and mass of clay biocomposite particles are denoted by v (L) and w (g) respectively [15].

For determination of pseudo first order model and pseudo second order, the following equations have been used:

$$\boldsymbol{log(q_e - q_t) = log(q_e) - \frac{k_1}{2.303}\, t} \qquad \text{Eq.}\,\mathbf{3}$$

The adsorbed sunset yellow at equilibrium is denoted by q_e (mg/g), while the quantity of sunset yellow adsorbed at time (t) is represented by q_t (mg/g). The rate constant of the pseudo first order model is represented by k_1 (min^{-1}). The $(q_e - q_t)$ plotted against the t whereas k_1 and q_e values were determined by using the slope and intercept of the plot respectively [16].

$$\frac{\mathbf{t}}{\mathbf{q_t}} = \frac{\mathbf{1}}{\mathbf{k_2 q_e}} + \frac{\mathbf{t}}{\mathbf{q_e}} \qquad \text{Eq.}\,\mathbf{4}$$

where $k_2 q_e$ (g/mg·min) represents the initial adsorption rate and k_2 is the pseudo-second-order rate constant ($g \cdot mg/g^{-1} \cdot min^{-1}$). The adsorbed sunset yellow at equilibrium is denoted by q_e (mg/g), while the quantity of sunset yellow adsorbed at time (t) is represented by q_t (mg/g). The values of q_e and k_2 can be obtained by a linear plot of t/q_t versus t [17].

2.2.2.3 Adsorption isothermal study

The various initial concentrations of sunset yellow (5, 10, 15, 20, 25, 30, 35, 40, and 50 mg/L) under 298 K were studied to find out the equilibrium isotherm of adsorption at an optimized time. Clay biocomposite (0.01 g) was mechanically shaken with different concentrations of sunset yellow solution

for 45 minutes [18]. As a parallel experiment, each experiment was repeated three times, with the result that was calculated as the average of the three. The binding capacity of sunset yellow at the equilibrium is defined as Q_e (mg/g) which was calculated by using the following equation:

$$\boldsymbol{Qe} = \frac{[(\mathbf{C_0} - \mathbf{C_e}) \times \boldsymbol{v}]}{\boldsymbol{w}} \quad \text{Eq. } \mathbf{5}$$

where Q_e (mg/g) indicates the binding capacity of clay biocomposite. The initial and equilibrium concentration of the sunset yellow solution are represented by C_0 (mg/L) and C_e (mg/L) respectively. v (L) represents the volume of sunset yellow solution, and the mass of clay biocomposite particles is denoted by w (g) [15].

For determination of Langmuir isotherm model and Freundlich isotherm model, the following equations have been used:

$$\frac{\mathbf{C_e}}{\mathbf{q_e}} = \frac{\mathbf{1}}{\mathbf{Q_m b}} + \frac{\mathbf{C_e}}{\mathbf{Q_m}} \quad \text{Eq. } \mathbf{6}$$

The maximum sorption capacity is represented by Q_m (mg·g^{-1}). b (L·mg^{-1}) is the Langmuir constant related to the energy of sorption. The adsorbed sunset yellow at equilibrium is denoted by q_e (mg/g) and the equilibrium concentration of the sunset yellow solution is represented by C_e (mg/L). The monolayer adsorption capacity and affinity of the adsorbent are related to the Langmuir constant Q_m and b, respectively. The linear plot of C_e/q_e against C_e is used to give the values of q_e and b from the slope and intercept [18].

$$\boldsymbol{log}\ \mathbf{q_e} = \boldsymbol{log}\ \mathbf{K_f} + \left(\frac{\mathbf{1}}{\boldsymbol{n}}\right) \boldsymbol{log}\ \mathbf{C_e} \quad \text{Eq. } \mathbf{7}$$

whereas K_f (mg·g^{-1}) is the Freundlich constant for adsorption capacity. The adsorbed sunset yellow at equilibrium is denoted by q_e (mg/g) and the equilibrium concentration of the sunset yellow solution is represented by C_e (mg/L). The 1/n value is the Freundlich constant for intensity. The value of n indicates favorable adsorption when $1 < n < 10$ and it is more favorable as $1/n < 1$ [18].

2.2.3 Statistical analysis

The analysis results were expressed as mean values, standard deviation (SD) and standard error (SE). Results obtained from pH study, adsorption kinetic study and adsorption isothermal study were subjected to one way analysis of variance (ANOVA) at 5 % of significance level. Means with a significant difference ($p < 0.05$) were compared using Tukey comparison test. The statistical significance was calculated based on 95 % of confidence level. Hence, ($p<0.05$) denoted that the model terms have a significant impact on the response. All of the statistical data were obtained from Microsoft Excel Version 2021 and Minitab 18 software.

3. Results and Discussion

3.1 Determination of functional group

The functional groups that present in the natural fiber of oil palm empty fruit bunch, EFB-based biochar and clay (Ca-montmorillonite) were determined using Fourier transform infrared (FTIR) spectrophotometer [Figure 1].

Figure 1: FTIR analysis of raw oil palm empty fruit bunch (REFB)

According to Figure 1, the adsorption peak at 10.29.978 cm^{-1} was represented to Si-O-Si stretch due to the presence of silica in the raw empty fruit bunch. The peaks between 1260 and 1000 cm^{-1} were attributed to silica-containing mineral yields or C-O stretching [19]. The adsorption peak at 1316.370 cm^{-1} was indicated to the presence of C-O stretch. A study stated that the C-O stretching vibration of the aryl-alkyl ether in lignin or the stretching of the β-glycosidic bond of the cellulose chain in raw empty fruit bunch (REFB) was specified to the adsorption peak at 1236.60 cm^{-1} [20]. Next, the adsorption peak of REFB at 1451.721 cm^{-1} was assigned to N-H bend. Amide groups were responsible for the peaks at 1637.74 cm^{-1} and 1466.49 cm^{-1} [19]. There was presence of C=O stretch in the raw oil palm empty fruit bunch at peak of 1707.083 cm^{-1}. Stretching of the carbonyl group by C=O was responsible for the peak at 1732 cm^{-1}. The uronic acids in hemicelluloses' xylan were responsible for this peak [21]. Adsorption peak at 2919.460 cm^{-1} and 3278.959 cm^{-1} were represented to the presence of H-C-H stretch and O-H stretch respectively. The stretching vibration of the (-OH) hydroxyl group was responsible for the broad and intense band at 3420.84 cm^{-1} while the C-H stretching vibration of the $-CH_3$ group was responsible for the absorption peaks between 2930 and 2850 cm^{-1} [19].

The functional groups that present in EFB-based biochar was determined FTIR. [Figure 2].

Figure 2: FTIR analysis of empty fruit bunch based biochar (EFB-based biochar)

By referring Figure 2, there was presence of C-H bend at 742.745 cm^{-1} caused by out of plane C-H bending [22]. Because the functional groups from REFB were vaporized as volatile materials when heat was applied to the sample, it was demonstrated that the majority of the adsorption peaks in EFBB were lost during the carbonization process. This indicated that the carbonization process had been successful and that all of the EFB had been completely converted to carbon [23]. In light of this, it is possible that the surface functional groups of EFBB could operate as active sites for interacting with an adsorbate [22]. Adsorption peak at 1210.691 cm^{-1} indicated the presence of C-O stretch by which a study has also stated that there was adsorption peak at 1007.92 cm^{-1} represents C-O stretching caused by the presence of phenols and alcohols [24]. C-C=C symmetric stretch was responsible for the adsorption peak at 1586.230 cm^{-1}. The strong band was seen at 1586.74 cm^{-1} when raw EFB was

converted into activated carbon, which might be the result of the extreme stretching of conjugated C=C in aromatic rings or oxygen-aromatic bonding in aromatic ether [18]. Adsorption peak at 3372.367 cm^{-1} was assigned to O-H stretch. There was presence of O-H stretching at 3365.43 cm^{-1} due to the EFB biochar's cellulose component [25].

The functional groups that present in clay (Ca-montmorillonite) were determined using FTIR [Figure 3].

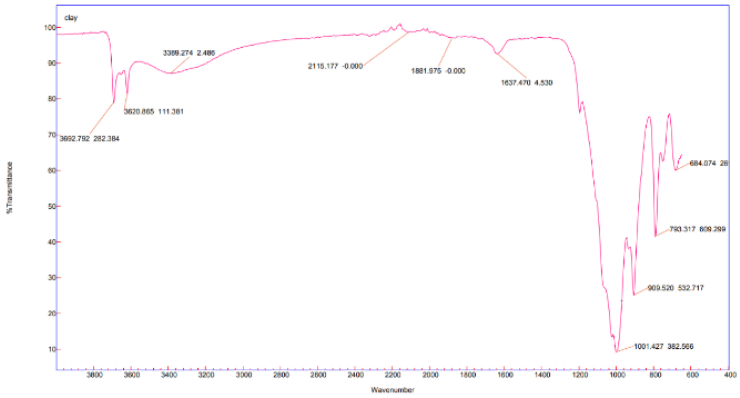

Figure 3: FTIR analysis of clay (Ca-montmorillonite)

According to Figure 3, adsorption peak at 909.520 cm^{-1} was represented to Al_2OH. Previous study has stated that at 916 cm^{-1}, the bands associated with the AlAlOH bending vibrations were seen [26]. Next, adsorption peak responsible for Si-O-Si group was observed at 1001.427 cm^{-1} due to the large number of silicas on montmorillonite clay surfaces. At 1040 cm^{-1}, a broad band associated to the stretching vibrations of Si-O groups [26]. C-C=C symmetric stretch was presented at 1637.470 cm^{-1} caused by an overtone of the bending vibration of water in montmorillonite [26]. Strong and broad band observed at 3620.865 and 3692.792 cm-1 were responsible for the O-H stretch. The stretching vibrations of the structural O-H groups of the montmorillonite were the cause of absorption band at a point of 3626 cm^{-1} [26].

3.2 Thermal analysis

The temperature of TGA analysis for raw empty fruit bunch (REFB) was ranged from 30 ℃ to 700 ℃ . There were three stages of REFB decomposition which include drying and evaporation of light components (first stage), devolatilization of cellulose and hemicellulose components (second stage) and decomposition of lignin (third stage). At the first stage, a minimal weight loss (14.548 %) was occurred for the REFB sample between 39.25 ℃ and 195.44 ℃ which was caused by the evaporation of moisture in REFB. A previous study has stated that similar trend most likely led to a 5% to 10% weight loss on the initial region of oil palm empty fruit bunch (OPEFB) fibers as a result of the water content evaporating. These alterations were related to cellulose's elimination of absorbed water [21]. At the second stage, there was 72.424 % of weight loss between 300.52 ℃ and 392.26 ℃. This results from a high rate of hemicellulose and cellulose degradation as well as the cleavage of cellulose's glyosidic links, which lowers the degree of polymerization and produces CO_2, H_2O, and a different type of hydrocarbon derivatives [21]. Weight loss of 95.121 % was occurred at third stage of REFB decomposition between 392.26 ℃ and 585.76 ℃ due to the loss of mass caused by decomposition of lignin content. The limit temperature for the decomposition of lignocellulosic components was determined from the thermogravimetric analysis to be 389.73 ℃ . Thus, the temperature for carbonization of EFB was chosen at 389.73 ℃ in order to be produced as biochar.

3.3 Effect of pH

The effect of pH solution on the amount of sunset yellow removed from water by EFB based biochar was observed by carrying out experiment at different pH values (4, 6, 8 and 10) with 10 mg/L of sunset yellow solution at 150 rpm for 120 minutes [Figure 4].

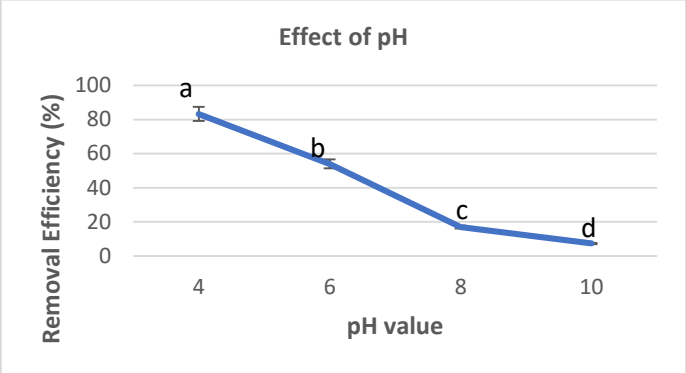

Figure 4: Effect of pH on the adsorption of sunset yellow

Figure 4 shows the plot of removal efficiency of sunset yellow in water against pH value. It can be observed that the removal efficiency of sunset yellow decreased as the pH value of the solution increased. At pH 4, the removal efficiency was accounted for 83.29% which indicating that maximum adsorption was occurred at lower pH value while at pH 6, the removal efficiency was started to decreased (54.01%). The adsorption of sunset yellow is significantly influenced by the pH of the solution. Adsorbent surfaces become protonated at acidic pH conditions, increasing the amount of dye adsorbed as a result of the electrostatic attraction between the positively charged surface and the negatively charged molecules of sunset yellow [27]. The removal efficiency was continued to decrease at pH 8 and pH 10 which were 16.91% and 7.32% respectively. This is due to the fact that as the pH of the adsorbate rises, fewer positively charged sites on the adsorbent are formed resulting in an increase in negative charges (OH^-) on the adsorbent, which reduces the anionic dyes' attraction to the surface of biochar. Since this situation prevents anionic dyes from being removed from the solution, electrostatic repulsion occurs [24]. The p-value obtained from statistical analysis was smaller than 0.05 ($p<0.05$) which means the null hypothesis was rejected and pH values have significant effect towards the adsorption study. All of the data obtained from pH study were significantly different from each other ($p<0.05$).

3.4 Effect of concentration

The effect of solution concentration on the percentage of sunset yellow removal by the adsorbent was investigated at various concentrations ranging from 5 mg/L to 50 mg/L [Figure 5].

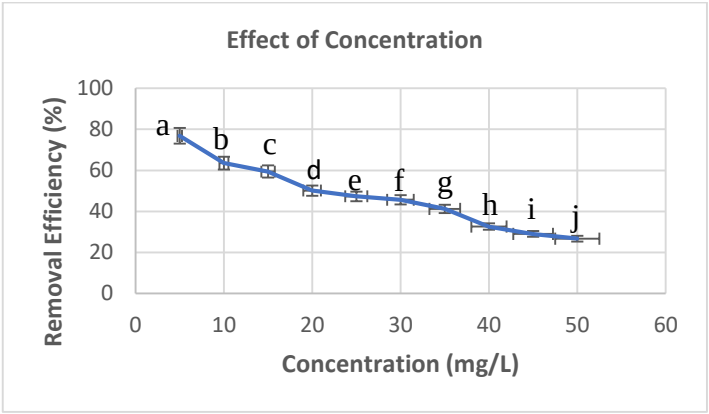

Figure 5: Effect of sunset yellow solution concentration

According to Figure 5, the adsorption decreased with increasing sunset yellow concentrations. The highest removal efficiency was observed at 5 mg/L (76.83%). The removal efficiency was 63.54%, 59.41%, 50.15%, 47.34%, 45.66%, 41.24%, 32.62%, 29.03% and 26.70% at 10, 15, 20, 25, 30, 35, 40,

45 and 50 mg/L respectively. Because there were enough active sites for interaction between the sunset yellow anions and the adsorbent at lower initial concentrations, the adsorbate was readily adsorbed on the surfaces of the adsorbent. The removal effectiveness decreases as the concentration rises because there were not enough adsorbent sites to completely bind the sunset yellow, which is impossible to do [28]. The p-value obtained from statistical analysis was smaller than 0.05 ($p<0.05$) which means the null hypothesis was rejected and concentration has significant effect towards the adsorption study. All of the data obtained from adsorption isothermal study were significantly different from each other ($p<0.05$).

3.5 Effect of contact time

Figure 3.7 shows a plot of removal efficiency against contact time. The effect of contact time was studied at different time intervals (2, 3, 5, 10, 15, 20, 25, 30, 40 and 50 minutes) [Figure 6].

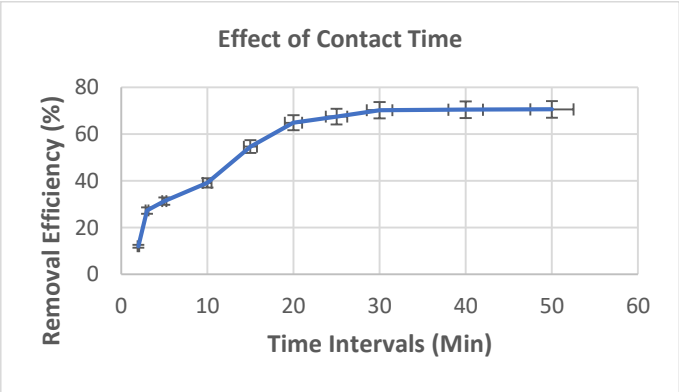

Figure 6: Effect of contact time between biochar and sunset yellow solution

The removal efficiency from 2 minutes to 30 minutes was increased whereas after 30 minutes the adsorption has become to an equilibrium state until 50 minutes. The study shows that the sunset yellow amount adsorbed by the biochar was increased with increasing contact time and the adsorption has reached equilibrium in 30 minutes. After 30 minutes, there was no any changes observed in the adsorption which caused the value of removal efficiency to remain constant. It was because of the binding sites on adsorbent have been saturated with sunset yellow anions causing no further occurrence of adsorption for more adsorbates. This result was aligned with the finding of previous study at which the removal efficiency increased with increasing time contact [27]. The adsorbent available sites approached toward saturation as the duration of treatment went on. After thirty minutes, equilibrium had been reached. Given that there are several adsorption sites, an increase in time causes an increase in the interaction between the contaminant and the larger surface area of the adsorbent.

3.6 Adsorption kinetic study

The adsorption mechanism of sunset yellow on EFB-based adsorbent was investigated by using pseudo-first order kinetic model and pseudo-second order kinetic model in linear form. Equations obtained from both graph plotting were $y= -0.0193x+0.8752$ and $y= 0.0682x+0.6141$ respectively. The k_1 value was -0.04445 while k_2 value was 0.11106. The coefficient of determination (R^2) of pseudo-second order kinetic model was bigger than pseudo-first order kinetic model which were 0.7068 and 0.9810 respectively. Therefore, Pseudo-second order kinetic model was the best fit to the experimental data. Previous study also obtained Pseudo-second order kinetic model as the best fit to the experimental data [24]. This ideal fit offered by Pseudo-second order kinetic model leads to the conclusion that both internal and exterior mass transfer processes played a significant role in the uptake of sunset yellow on EFB based adsorbent and that chemisorption may be the step that determines the rate of the sorption process [24].

3.7 Adsorption isotherm study

The adsorption mechanism of sunset yellow on EFB-based adsorbent was investigated by using Langmuir isotherm model and Freundlich isotherm model in linear form. Equations obtained from both graph plotting were y= 0.0703x+0.0817 and y= 0.31x+0.7289 respectively. The Langmuir constant was 0.8605 and the Freundlich constant was 5.3567. The coefficient of determination (R^2) of Langmuir isotherm model was bigger than Freundlich isotherm model which were 0.9598 and 0.7737 respectively. Therefore, Langmuir isotherm model was the best fit to the experimental data. The Langmuir isotherm was the best defined of the adsorption of sunset yellow on MCM-41 (Mobil Composition of Matter No. 41), showing that the adsorption was homogenous and that a monolayer was present [29]. Data of a study about the adsorption of sunset yellow azo dye on activated carbon entrapped in alginate were fitted with the Langmuir isotherm [27].

4. Conclusion

Oil palm empty fruit bunch-based biochar was capable to eliminate the sunset yellow concentration in water. The surface properties of raw empty fruit bunch (REFB), biochar and clay was determined through FTIR in the range of 400 to 4000 cm^{-1}. Different operating factors on the efficiency of sunset yellow removal were investigated. The experimental variables, such as solution pH, concentration, and contact time, had an impact on the removal. At pH 4, a higher elimination efficiency was observed with 10 mg/L of sunset yellow solution concentration, 10 mg of adsorbent dosage, 150 rpm of stirring speed and 120 minutes of contact time. The effectiveness of sunset yellow removal from water was decreased as the concentration of the solution increased. The removal efficiency decreased from76.83% to 26.70% as the concentration of solution increased from 5 mg/L to 50 mg/L with 10 mg of adsorbent dosage, 150 rpm of stirring speed and 45 minutes of contact time. The removal efficiency of sunset yellow was increased as the contact time between the adsorbent and the adsorbate increased. After 30 minutes of adsorption, the removal efficiency reached equilibrium. The Langmuir isotherm model and the pseudo-second order kinetic model had the best fit to the adsorption data, with coefficient of determination of 0.9598 and 0.981 respectively. There are few recommendations that could be implemented for further research. Other parameters such as stirring speed, temperature and adsorbent dosage should be examined in depth to investigate its effects on the adsorption of sunset yellow and come up with most effective reference for the treatment of wastewater that contain sunset yellow residues from food industries. Adsorption method using biocomposite is one of the inexpensive alternatives for the waste water treatment.

Acknowledgement

For the lab work and facilities offered for the research, the authors are grateful to the Faculty of Applied Sciences and Technology at Universiti Tun Hussein Onn Malaysia.

References

[1] Ponomarev, A. v., Kholodkova, E. M., & Bludenko, A. v. (2022). Radiolytic decolouration of aqueous solutions of food dyes. Radiation Physics and Chemistry, 199. https://doi.org/10.1016/j.radphyschem.2022.110357

[2] Benkhaya, S., M'rabet, S., El Harfi, A., 2020. A review on classifications, recent synthesis and applications of textile dyes. Inorganic Chemistry Communications, 115, 107891.

[3] Alizadeh, M., Demir, E., Aydogdu, N., Zare, N., Karimi, F., Kandomal, S.M., Rokni, H., Ghasemi, Y., 2022. Recent advantages in electrochemical monitoring for the analysis of amaranth and carminic acid food colors. Food and Chemical Toxicology, 112929.

[4] Jiang, R., Shen, T. T., Zhu, H. Y., Fu, Y. Q., Jiang, S. T., Li, J. B., & Wang, J. L. (2022). Magnetic Fe3O4 embedded chitosan–crosslinked-polyacrylamide composites with enhanced

removal of food dye: Characterization, adsorption and mechanism. International Journal of Biological Macromolecules. https://doi.org/10.1016/j.ijbiomac.2022.11.310

[5] Songyang, Y., Yang, X., Xie, S., Hao, H., Song, J. (2015). Highly–sensitive and rapid determination of sunset yellow using functionalized montmorillonite–modified electrode, Food Chemistry, 173, 640–644.

[6] Chukwuemeka-Okorie, H. O., Ekuma, F. K., Akpomie, K. G., Nnaji, J. C., & Okereafor, A. G. (2021). Adsorption of tartrazine and sunset yellow anionic dyes onto activated carbon derived from cassava sievate biomass. Applied Water Science, 11(2). https://doi.org/10.1007/s13201-021-01357-w

[7] Okeola, F. O., Odebunmi, E. O., Ameen, O. M., Amoloye, M. A., Lawal, A. A. , Abdulmummeen, A. G. (2017). Equilibrium kinetics and thermodynamic studies of the adsorption of tartrazine and sunset yellow. Arid Zone Journal of Engineering, Technology and Environment, 13(2):268–280.

[8] Lau, K. T., Ho, M. P., Au-Yeung, C. T., & Cheung, H. Y. (2010). Biocomposites: Their multifunctionality. *International Journal of Smart and Nano Materials*, *1*(1), 13–27. https://doi.org/10.1080/19475411003589780

[9] Kausar, A. (2017). Role of thermosetting polymer in structural composite. *American Journal of Polymer Science and Engineering*, *5*, 1–12.

[10] Alamri H, Low IM. (2012). Mechanical properties and water absorption behaviour of recycled cellulose fibre reinforced epoxy composites. Polymer Testing, 31(5):620–628.

[11] Villain G, Thiery M, Platret G. (2007). Measurement methods of carbonation profiles in concrete: Thermogravimetry, chemical analysis and gammadensimetry. Cement and Concrete Research, 37, 1182–1192.

[12] Munir S, Daood SS, Nimmo W, Cunliffe AM, Gibbs BM. (2009). Thermal analysis and devolatilization kinetics of cotton stalk, sugar cane bagasse and shea meal under nitrogen and air atmospheres. Bioresource Technology, 100(3):1413–8.

[13] Kausar, A., Shahzad, R., Iqbal, J., Muhammad, N., Ibrahim, S. M., & Iqbal, M. (2020). Development of new organic-inorganic, hybrid bionanocomposite from cellulose and clay for enhanced removal of Drimarine Yellow HF-3GL dye. International Journal of Biological Macromolecules, 149, 1059–1071. https://doi.org/10.1016/j.ijbiomac.2020.02.012

[14] Mohammadi, N.; Khani, H.; Gupta, V.K.; Amereh, E.; Agarwal, S.J.J.o.c.; science, i. (2011). Adsorption process of methyl orange dye onto mesoporous carbon material–kinetic and thermodynamic studies. 362, 457-462.

[15] Asman, S., Mohamad, S., & Sarih, N. M. (2016). Study of the morphology and the adsorption behavior of molecularly imprinted polymers prepared by reversible addition-fragmentation chain transfer (RAFT) polymerization process based on two functionalized β-cyclodextrin as monomers. Journal of Molecular Liquids, 214, 59–69. https://doi.org/10.1016/j.molliq.2015.11.057

[16] Ho, Y. S., & Mckay, G. (1999). Pseudo-second order model for sorption processes. In Process Biochemistry (Vol. 34).

[17] Ahmed, M. J., & Dhedan, S. K. (2012). Equilibrium isotherms and kinetics modeling of methylene blue adsorption on agricultural wastes-based activated carbons. Fluid Phase Equilibria, 317, 9–14. https://doi.org/10.1016/j.fluid.2011.12.026

[18] Surikumaran, H., Mohamad, S., & Sarih, N. M. (2014). Molecular imprinted polymer of methacrylic acid functionalised β-Cyclodextrin for selective removal of 2,4-dichlorophenol.

International Journal of Molecular Sciences, 15(4), 6111–6136. https://doi.org/10.3390/ijms15046111

[19] Wirasnita, R., Hadibarata, T., Yusoff, A. R. M., & Yusop, Z. (2014). Removal of bisphenol a from aqueous solution by activated carbon derived from oil palm empty fruit bunch. Water, Air, and Soil Pollution, 225(10). https://doi.org/10.1007/s11270-014-2148-x

[20] Radzi, N. A. M., Sofian, A. H., & Jamari, S. S. (2020), Structural Studies of Surface Modified Oil Palm Empty Fruit Bunch with Alkaline Pre-treatment as a Potential Filler for the Green Composite, Jurnal Tribologi, 26(1), 75-83.

[21] Ramlee, N. A., Jawaid, M., Zainudin, E. S., & Yamani, S. A. K. (2019). Modification of Oil Palm Empty Fruit Bunch and Sugarcane Bagasse Biomass as Potential Reinforcement for Composites Panel and Thermal Insulation Materials. Journal of Bionic Engineering, 16(1), 175–188. https://doi.org/10.1007/s42235-019-0016-5

[22] Hadibarata, T., Wirasnita, R., Yusoff, A. R. M., & Lazim, Z. M. (2015), Preparation and Characterization of Activated Carbon from Oil Palm Empty Fruit Bunch Wastes using Zinc Chloride, Jurnal Teknologi, 74(11), 77-81.

[23] Hidayu, A. R., Mohamad, N. F., Matali, S., & Sharifah, A. S. A. K. (2013), Characterization of Activated Carbon Prepared from Oil, Palm Empty Fruit Bunch using BET and FT-IR Techniques, Procedia Engineering, 68(1), 379- 384.

[24] Chukwuemeka-Okorie, H. O., Ekuma, F. K., Akpomie, K. G., Nnaji, J. C., & Okereafor, A. G. (2021). Adsorption of tartrazine and sunset yellow anionic dyes onto activated carbon derived from cassava sievate biomass. Applied Water Science, 11(2). https://doi.org/10.1007/s13201-021-01357-w

[25] Sari, N. A., Ishak, C. F., & Bakar, R. A. (2014). Characterization of oil palm empty fruit bunch and rice husk biochars and their potential to adsorb arsenic and cadmium. American Journal of Agricultural and Biological Science, 9(3), 450–456. https://doi.org/10.3844/ajabssp.2014.450.456

[26] Danková, Z., Mockovčiaková, A., & Dolinská, S. (2014). Influence of ultrasound irradiation on cadmium cations adsorption by montmorillonite. Desalination and Water Treatment, 52(28–30), 5462–5469. https://doi.org/10.1080/19443994.2013.814006

[27] Abdel-Aziz, H. M., & Abdel-Gawad, S. A. (2020). Removal of sunset YellowAzo dye using activated carbon entrapped in alginate from aqueous solutions. https://doi.org/10.15406/oajs.2020.04.00142

[28] Ghahremani, A., Manteghian, M., & Kazemzadeh, H. (2021). Removing lead from aqueous solution by activated carbon nanoparticle impregnated on lightweight expanded clay aggregate. Journal of Environmental Chemical Engineering, 9(1). https://doi.org/10.1016/j.jece.2020.104478

[29] Oguz Erdogan, F., & Erdogan, T. (2018). Adsorption Of Sunset Yellow Fcf Onto MCM-41. www.tojsat.net